ORIGINAL PAPER

Reduction of Substituted *p*-Benzoquinones by Fe^{II} Near Neutral pH

Minori Uchimiya · Alan T. Stone

Abstract The oxidation of dihydroxyaromatics to benzoquinones by Fe^{III} (hydr)oxides is important in respiratory electron shuttling by microorganisms and has been extensively studied. Prior publications have noted that the Gibbs Free Energy (ΔG) for the forward reaction is sensitive to dihydroxyaromatic structure, pH, and concentrations of reactants and products. Here, we address the back reaction, benzoquinone reduction by Fe^{II}. Rates markedly increase with increasing pH, in accord with increases in ΔG. Ring substituents that raise the potential of the *p*-benzoquinone/hydroquinone half reaction raise reaction rates: $-OCH_3 < -CH_3 < -C_6H_5 < -H < -Cl$. *p*-Naphthoquinone, with a reduction potential lower than the five substituted *p*-benzoquinones just listed, yields the lowest reaction rates. The complexity of the reaction is reflected in lag periods and less-pronounced S-shaped time course curves. Benzoquinone reduction by Fe^{II} may be an important link in networks of electron transport taking place in suboxic and anoxic environments.

Keywords Ferrous ion · Hydroquinones · Benzoquinones · Kinetics · Electron transfer

1 Introduction

Oxidations of dihydroxybenzenes to benzoquinones and corresponding back reactions are often reversible under neutral and acidic conditions, earning them a prominent place in organic electron transfer chemistry. Several lines of evidence indicate that benzoquinones/ dihydroxybenzenes may be biogeochemically important as well. Hydroxyaromatic-rich

M. Uchimiya
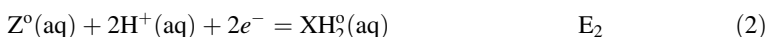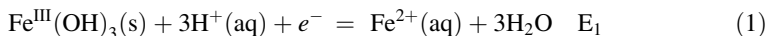USDA-ARS, 1100 Robert E. Lee Boulevard, New Orleans, LA 70124, USA

A. T. Stone (✉)
Department of Geography and Environmental Engineering, 313 Ames Hall, Johns Hopkins University, Baltimore, MD 21218, USA
e-mail: astone@jhu.edu

lignin is an important precursor of natural organic matter (NOM) of terrestrial origin. Electrochemistry (Nurmi and Tratnyek 2002; Fimmen et al. 2007) and microbial action (Scott et al. 1998) have been used to cycle NOM between oxidized and reduced forms, believed to be benzoquinone/dihydroxybenzene moieties. Changes in fluorescent spectra are consistent with this conclusion (Klapper et al. 2002; Cory and McKnight 2005). Aniline forms adducts with NOM that yield ^{15}N NMR spectra most consistent with Michael-type nucleophilic attack onto benzoquinone moieties (Thorn et al. 1996). Semiquinone radicals, generated by one-electron reduction in benzoquinones, one-electron oxidation of dihydroxybenzenes, and benzoquinone–hydroquinone comproportionation (Alegria et al. 1996), are observable in NOM samples using ESR (Senesi and Steelink 1989; Paul et al. 2006).

Plant-, fungus-, and bacteria-derived benzoquinones and dihydroxybenzenes with antibiotic and allelochemical properties are well known. Lawsone, juglone (Schwarzenbach et al. 1990), and sorgoleone (Chang et al. 1986) are illustrative examples. The prevailing view is that these molecules enter cells of target organisms, where they interfere with biological electron transport and energy fixation/utilization (von Jagow and Link 1986; Gonzalez et al. 1997; Hejl and Koster 2004). Outside of cells, benzoquinones and dihydroxybenzenes may serve as signaling compounds and indicators of prevalent redox conditions. Bacterial redox taxis in response to benzoquinone and dihydroxybenzene concentration gradients has been observed (Bespalov et al. 1996). Since benzoquinones and dihydroxybenzenes elicit different biological responses, understanding their redox interconversion is important.

The possibility that benzoquinones and dihydroxybenzenes may facilitate microbial Fe^{III} respiration has received a great deal of attention. Bacterial terminal reductases are membrane bound, and Fe^{III} (hydr)oxides are sparingly soluble near neutral pH. Two mechanisms for respiration in the absence of physical contact have been hypothesized. The first mechanism relies upon strong chelating agents to solubilize and transport Fe^{III}. Chelation lowers the $Fe^{III/II}$ reduction potential, however, lowering the metabolic gain (Arnold et al. 1986). Replacing relatively weak chelating agents with stronger ones lowers Fe^{II} production rates (Haas and DiChristina 2002). The second mechanism employs an oxidant/reductant pair to shuttle electrons between Fe^{III} (hydr)oxides and cell membranes (Lies et al. 2005). AQDS and the naphthoquinones lawsone and menadione (Lovley et al. 1998; Newman and Kolter 2000) are known to serve in this role, along with nitrogen-containing analogs to benzoquinones, the phenazines (Hernandez et al. 2004). Electron shuttling using naphthoquinone/ p-dihydroxynaphthalene half reaction is illustrated in Fig. 1. Bacteria capable of using the synthetic p-benzoquinone compound AQDS as the sole electron acceptor are readily isolated (Cervantes et al. 2003). NOM, presumably because of the benzoquinone/dihydroxybenzene moieties it possesses, also facilitates respiration (Lovley et al. 1996; Coates et al. 1998; Lovley et al. 1999; Jiang and Kappler 2008).

To further explore reaction energetics, consider the half reactions for Fe^{III}/Fe^{II} and benzoquinone/dihydroxybenzene interconversions:

$$Fe^{III}(OH)_3(s) + 3H^+(aq) + e^- = Fe^{2+}(aq) + 3H_2O \quad E_1 \tag{1}$$

$$Z^o(aq) + 2H^+(aq) + 2e^- = XH_2^o(aq) \qquad\qquad E_2 \tag{2}$$

We have elected to use a solubility product of $^*K_{so} = 10^{+3.0}$ for the reaction $Fe^{III}(OH)_3(s) + 3H^+(aq) = Fe^{3+}(aq) + 3H_2O$, which is within the range for ferrihydrite/ amorphous $Fe^{III}(OH)_3(s)$ offered by Majzlan et al. (2004). (We use $^*K_{so} = 10^{+12.88}$ for the $Fe^{II}(OH)_2(s) + 2H^+ = Fe^{2+}(aq) + 2H_2O$ reaction (Martell et al. 2004). $Fe^{II}(OH)_2(s)$ only
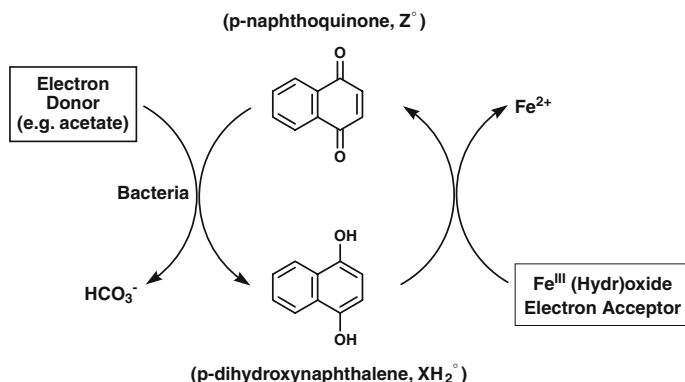
Fig. 1 Bacteria physically separated from Fe^{III} (hydr)oxide surfaces can perform iron respiration provided that a suitable electron shuttle is present, represented here by the *p*-naphthoquinone/*p*-dihydroxynaphthalene half reaction

precipitates at pHs greater than 8). $XH_2^o(aq)$ represents each dihydroxybenzene, and $Z^o(aq)$ represents each benzoquinone. The two half reactions can be combined to yield the overall reaction stoichiometry:

$$XH_2^o(aq) + 2Fe^{III}(OH)_3(s) + 4H^+(aq) \rightarrow Z^o(aq) + 2Fe^{2+}(aq) + 6H_2O$$
$$\Delta G = -2F(E_1 - E_2) \tag{3}$$
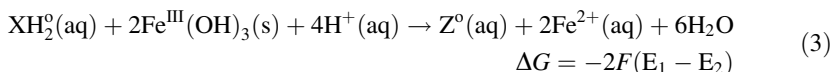
The left hand portion of the cycle shown in Fig. 1 is energetically favorable, because the reduction potential for enzyme-catalyzed conversion of organic electron donors to inorganic carbonate is quite low, and the reduction potential for the benzoquinone/dihydroxybenzene interconversion is relatively high. The right hand portion of the cycle requires that the reduction potential for the Fe^{III}/Fe^{II} half reaction (E_1) be higher than that for the benzoquinone/dihydroxybenzene half reaction (E_2), such that ΔG for Reaction 3 is negative.

Suppose that 100 μmol of $Fe^{III}(OH)_3(s)$ has been added to a liter of solution to serve as electron acceptor. 50 μM hydroquinone, *p*-dihydroxynaphthalene, or the fully reduced form of AQDS are then added. The lines drawn in Fig. 2 correspond to the point in each reaction where exactly half of each dihydroxybenzene has been oxidized. Under these constraints, the reduced form of AQDS yields energetically favorable $Fe(OH)_3(s)$ reduction at all pHs below 8.25. With *p*-dihydroxynaphthalene, the pH must be below 6.38, and with hydroquinone, the pH must be below 4.46. Note that the pH range where the scheme shown in Fig. 1 is operative can be extended if the conditions are appropriately adjusted, i.e., if the concentration of $Fe^{2+}(aq)$ is lowered while keeping the activity of the $Fe^{III}(OH)_3(s)$ fixed or if the concentration of the dihydroxybenzene is raised relative to the corresponding benzoquinone. Near neutral pH, three-ring and possibly two-ring benzoquinones/dihydroxybenzenes are suitable electron shuttling compounds. Single-ring compounds are unlikely candidates.

Figure 2 also provides the means of investigating the energetics of the back reaction, $Fe^{2+}(aq)$ oxidation by benzoquinones:
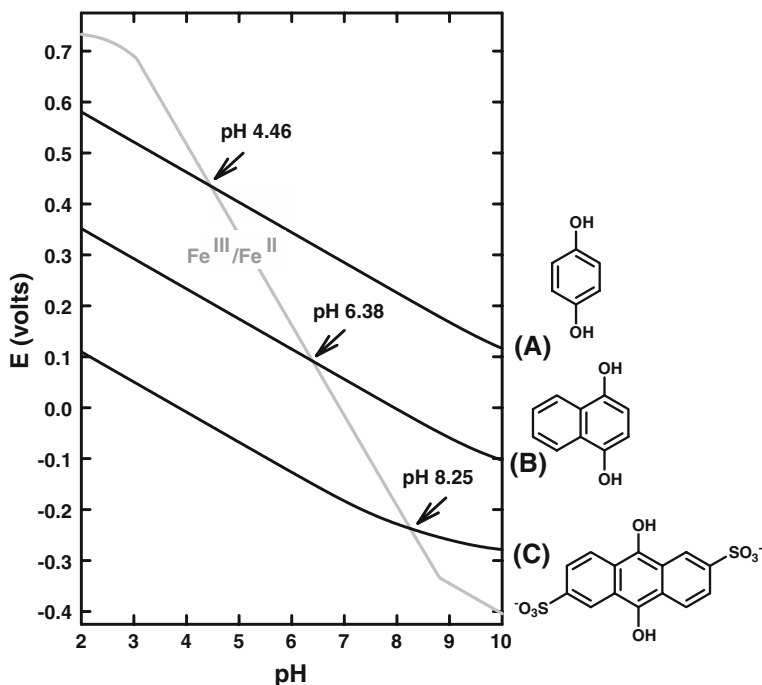
$$Z^o(aq) + 2Fe^{2+}(aq) + 6H_2O \rightarrow XH_2^o(aq) + 2Fe^{III}(OH)_3(s) + 4H^+(aq)$$
$$\Delta G = -2F(E_2 - E_1) \tag{4}$$
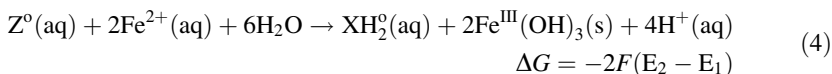
Fig. 2 Reduction potentials calculated for the point where 50% of *a* hydroquinone, *b* p-dihydroxynaph-thalene, and *c* the reduced form of AQDS have been oxidized to the corresponding p-benzoquinone by Fe(OH)$_3$(s). Initial conditions: 50 µM dihydroxybenzene, 100 µM Fe(OH)$_3$(s), and 0.10 M NaCl. Fe(OH)$_3$(s) (*K_{so} = 10$^{+3.00}$) is employed as the Fe^{III} solubility-limiting phase

Under the conditions selected for Fig. 2, ΔG is favorable for Fe^{2+}(aq) oxidation by *p*-benzoquinone at pHs above 4.46, for oxidation by *p*-naphthoquinone above 6.38, and for oxidation by AQDS above 8.25.

Figure 3a presents calculated ΔG values for Reaction 4 as a function of the concentration of *p*-benzoquinone reduced, which serves as our reaction progress variable. ΔG values are calculated using the following equation:

$$\Delta G = -2F(E_2 - E_1) = \Delta G^o + RT \ln \left(\frac{\{XH_2^o(aq)\} a_{Fe(OH)_3}^2 \{H^+\}^4}{\{Z^o(aq)\}\{Fe^{2+}(aq)\}^2} \right) \qquad (5)$$

ΔG^0 is the Standard Gibbs Free Energy of Reaction 4, i.e., mole fractions of water and solid phases equal to 1.0 and activities of all solutes equal to 1.0 M. R is the gas constant, and T is the temperature, in Kelvin. ΔG is asymptotically negative at the onset of reaction, since the hydroquinone concentration is equal to zero when the reaction progress variable is equal to zero. As the reaction approaches completion, ΔG becomes asymptotically positive, reflecting *p*-benzoquinone and Fe^{2+}(aq) concentrations that approach zero. Overall, S-shaped curves are seen, which shift toward more negative ΔG values as the pH is increased. The point within each curve where $\Delta G = 0$ corresponds to the final, equilibrium state, beyond which reaction is no longer energetically favorable. Higher pH makes conversion of a larger amount of *p*-benzoquinone into hydroquinone energetically possible.

Figure 3b illustrates the effects of adding 1.0, 5.0, and 10 μM of the reaction product hydroquinone at the onset of reaction. Note that the early asymptote disappears. The biggest lowering of ΔG accompanying hydroquinone addition takes place early in the reaction. The effect diminishes as additional hydroquinone generated by p-benzoquinone reduction accumulates in the system.

Prior studies of Fe^{2+}(aq) oxidation by benzoquinones employed strongly acidic conditions to avoid the formation of Fe^{III} (hydr)oxide precipitates and high concentrations of reactants relative to products to ensure that forward reaction is energetically favorable (Porret 1934; Baxendale et al. 1951; Baxendale and Hardy 1955; Mentasti et al. 1973). Reaction 4 has been mentioned as a contributing factor in the oxidation of adrenaline in solutions containing O_2 and Fe^{2+}(aq) (Linert et al. 1993) and the oxidation of dopamine in solutions containing linoleic acid 13-hydroperoxide and Fe^{2+}(aq) (Pezzella et al. 1997).

Benzoquinones have been implicated in at least one biochemical pathway for microbial Mn^{2+}(aq) oxidation (Johnson and Tebo 2008). Since the reduction potential for the Fe^{III}/ Fe^{II} half reaction is substantially lower than that of the Mn^{III}/Mn^{II} half reaction, Fe^{2+}(aq) oxidation via the same microbial pathway should be energetically favorable.

The present work investigates the oxidation of Fe^{2+}(aq) by p-benzoquinones under strictly anoxic conditions at pHs relevant to natural aquatic environments. p-Benzoquinones with electron-donating and electron-withdrawing substituents serve as useful probes of reaction mechanism. Depending upon the pH and initial reactant concentrations employed, the thermodynamic driving force for reaction (ΔG) may reach zero before 50% or more of the limiting reactant has been consumed.

2 Materials and Methods

Unless otherwise stated, Milli-Q water (18 MΩ·cm resistivity; Millipore Corp., Milford, MA) was used to prepare all stock and reaction solutions. All chemicals were purchased from suppliers at the highest purity available and were used as received. All glass and
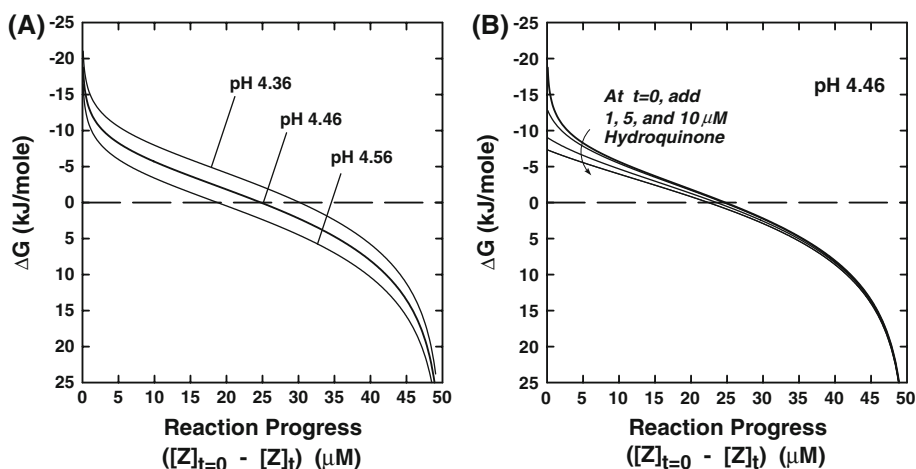

Fig. 3 Gibbs Free Energy (ΔG) as a function reaction progress calculated for the reduction in 50 μM p-benzoquinone (Z) by 100 μM Fe^{II} in 0.10 M NaCl medium. a Focuses on three pHs near the crossover point in Fig. 1. b illustrates the effect of adding 1.0, 5.0, and 10 μM hydroquinone at the onset of reaction

plasticware were first rinsed with acetone (J.T. Baker, Phillipsburg, NJ), and then with distilled water, prior to being soaked in a 5.0 M nitric acid (J.T. Baker) bath overnight. Acid-washed glass and plasticware was rinsed three times with Milli-Q water and air-dried prior to use. Glass- and plastic-ware having prior contact with metal ions were soaked in a 5.0 mM oxalic acid (Aldrich Chemical Co., Milwaukee, WI) bath at 30°C overnight, before following the above procedure.

Methoxybenzoquinone and α-naphthoquinone (1,4-) were purchased from TCI America (Portland, OR). Naphthohydroquinone, phenylhydroquinone, hydroquinone, methoxyhy-droquinone, methylhydroquinone, chlorohydroquinone, 1,4-benzoquinone, 2-chloro-1,4-benzoquinone, 2-methyl-1,4-benzoquinone, and phenyl-p-benzoquinone, and disodium ethylenediaminetetraacetate (EDTA) were purchased from Aldrich.

2.1 Experimental Setup

A controlled-atmosphere glovebag (95% N_2, 5% H_2, Pd catalyst, Coy Laboratory Products, Grass Lake, MI) was used to maintain strict O_2-free conditions. A constant temperature bath within the glovebag was used to maintain all experiments at 25°C. All stock and reaction solutions were prepared using autoclaved, N_2-sparged (BOC gases, Baltimore, MD) Milli-Q water within the glove bag. All organic stock solutions were filtered (0.22-μm pore diameter, Millex-GS filters, Millipore Corp., Billerica, MA) prior to use. Stock solutions of 1.0 mM benzoquinone in 1.0 mM HCl were prepared daily and were stored in the dark. Benzoquinones with low aqueous solubility were first dissolved in methanol (J.T. Baker, Phillipsburg, NJ). The volume fraction of methanol in the reaction solution was kept below 1.0%. Control experiments demonstrated that methanol yielded negligible effects on reaction rate at volume fractions below 5.0%.

A stock solution of 1.0 M $FeCl_2$/1.0 mM HCl was prepared by dissolving $FeCl_2 \cdot 4H_2O$ (Aldrich) in neutral Milli-Q water and filtering with a 0.02-μm pore diameter inorganic alumina-matrix membrane filter (Anotop, Whatman Scientific, Maidstone, England) to remove trace Fe^{III}, followed by acidification using HCl. A stock solution of 1.0 M $FeCl_3$/1.0 mM HCl was prepared by dissolving $FeCl_3 \cdot 3H_2O$ (Aldrich) in acidified solution. Iron stock solution concentrations were determined using flame atomic absorption spectro-photometry (AAS; Analyst 100, Perkin-Elmer, Norwalk, CT).

All reactions were performed in 125-mL polypropylene containers, each with contin-uously rotating teflon-coated stir bar. To minimize experiment-to-experiment variations in ionic strength, 0.10 M NaCl (Aldrich) was employed. pH values less than or equal to 3.0 were set by HCl (Aldrich) addition. Sodium acetate (pK_a 4.76) was used to fix pH within the range $3.0 \leq pH < 5.5$. 2-(N-Morpholino)ethanesulfonic acid monohydrate (MES; pK_a 6.15) was employed in the range $5.5 \leq pH < 6.5$. 3-(N-Morpholino)-propanesulfonic acid (MOPS; pK_a 7.20) was employed in the range $6.5 \leq pH < 8.0$. The organic buffers employed, all obtained from Aldrich, exhibit negligible metal ion-coordinating ability (Good et al. 1966; Good and Izawa 1972).

At selected time intervals, aliquots were filtered (Anotop 25-Plus inorganic 0.02-μm membrane filter; Whatman) and then syringe-injected through a short cation exchange resin-filled column (OnGuard-H; Dionex Corp., Sunnyvale, CA). Fe^{II} and Fe^{III} were both removed using this procedure, quenching reaction. All samples were tightly capped in glass vials (15 mm × 44 mm screw thread clear vials, Fisher Scientific) prior to removal from the glove bag and subsequent HPLC analysis. After each sample collection, reaction solution pH was measured using a Fisher Accumet 825 MP meter with Orion combination semi-micro probe calibrated using NIST-traceable standards.

2.2 HPLC Analysis

A two-pump HPLC system with autosampler and UV detector (Waters Corp., Milford, MA) was run in isocratic mode with a total flow rate of 1 mL min^{-1}. Separation was achieved using a 3.9 mm × 300 mm 10-μm C_{18} column (μBondapakTM WATO27324, Waters Corp.) plus pre-column insert (GuardPak, Waters Corp.). Depending upon the analytes under investigation, different ratios of (1) either methanol or acetonitrile (J.T. Baker) and (2) 5.0 mM acetic acid were employed as eluent. Both organic and aqueous solvents were filtered (membrane filters with 0.45 mm pore size; Millipore, Billerica, MA) and degassed for more than 30 min prior to use. No additional efforts were made to remove O_2 from HPLC solvents.

Detection limits, defined as the minimum analyte concentration affording signal-to-noise ratios greater than 3.0, were below 5.0 μM for dihydroxybenzenes and for benzoquinones. HPLC analysis revealed that 50 μM benzoquinone solutions prepared from stock solutions contained trace amounts of dihydroxybenzenes (mean ± standard deviation for 5 samples): 1.1 ± 0.7 μM for *p*-benzoquinone; 7.7 ± 2.6 μM for 2-chloro-*p*-benzoquinone; 4.7 ± 0.3 μM for 2-methyl-*p*-benzoquinone; and 4.6 ± 0.2 μM for phenyl-*p*-benzoquinone. Hydroquinone contamination in methoxy-*p*-benzoquinone and *p*-naphthoquinone stock solutions was below our detection limit.

2.3 Preparation of a Fe^{III} (Hydr)oxide Standard Suspension

Fe^{III} (hydr)oxide particles generated by the reaction of 250 μM Fe^{II} with 50 μM *p*-benzoquinone at pH 5.9 (50 mM MES buffer, 0.10 M NaCl) were characterized using transmission electron microscopy (TEM). After 1 h of reaction, the particles were collected using 0.2-μm polycarbonate track etch membrane filters (Whatman), washed with 200 mL Milli-Q water, and sonicated in 20 mL Milli-Q water for 1 h. A holey-carbon grid was dipped into the suspension and dried within the glove bag. The grid was then inserted into a Philips 420T TEM for analysis. Images revealed crumpled sheet-like structures that were approximately 5-nm thick. Some of the sheets appeared as disk-like structures 100 to 200 nm in diameter. Electron diffraction revealed a powder pattern with 3.4, 2.1, 1.2, 1.1, 0.81, and 0.72 Angstrom d-spacings.

3 Results

3.1 *p*-Benzoquinone Reduction

All experiments employed 50 μM benzoquinone and 250 μM Fe^{II}. According to Reaction 4, this represents a 2.5-fold stoichiometric excess of Fe^{II}. In each experiment, the pH was set high enough to ensure that > 90% conversion of benzoquinone reactant into dihydroxybenzene product was energetically favorable. (Calculations were performed using Eq. 5 and plotted in the manner illustrated in Fig. 3.)

The uppermost plot in Fig. 4 shows the time course obtained upon addition of 50 μM *p*-benzoquinone to a solution containing 250 μM Fe^{II}, 50 mM MES buffer (pH 5.9), and 0.10 M NaCl. A distinctive lag period, lasting approximately 9 min, was observed. Subsequent to this lag period, a steady hydroquinone production matched *p*-benzoquinone consumption. Mass balance was obtained. Half of the initial *p*-benzoquinone concentration was consumed within the first 15 min of reaction.

Based upon HPLC analysis of Fe-free control solutions at this pH, it is likely that approximately 1 μM hydroquinone was present at the onset of the reaction just described. To explore the effect that this reaction product might have on kinetics, additional experiments (Fig. 4b–d) were performed which employed increasing amounts of hydroquinone stock solution. Lag periods became increasing harder to discern as 1.0, 5.0, and 10 μM hydroquinone stock solutions were added. The clear break in slope at approximately 9 min cannot be seen. The time required for consumption of half of the added p-benzoquinone rose to 23, 32, and 53 min, respectively.

An additional experiment investigated whether the other reaction product, precipitated Fe^{III} (hydr)oxides, affected the reaction time course. In Fig. 5a, an Fe^{III} (hydr)oxide loading of 94 μM was employed, using the stock suspension described in Materials and Methods. Initial Fe^{II} concentration, p-benzoquinone concentration, and pH were the same
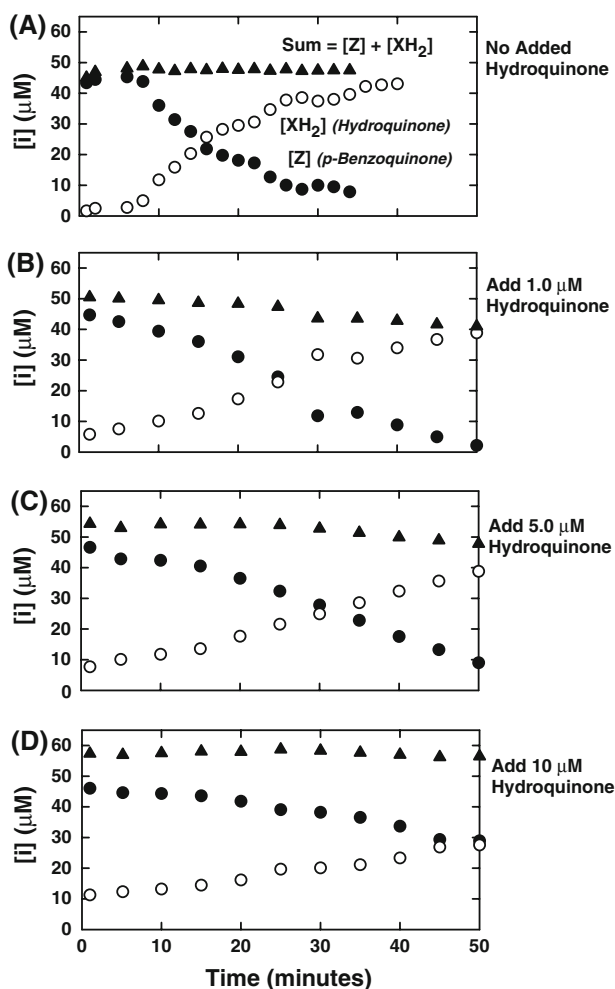

Fig. 4 **a** Time course plot for the reduction in 50 μM p-benzoquinone by 250 μM Fe^{II} at pH 5.9 (50 mM MES pH buffer, 0.10 M NaCl). (**b–d**) Effect of adding 1.0, 5.0, and 10 μM hydroquinone at the onset of the reaction

as in Fig. 4a. Adding Fe^{III} (hydr)oxide particles had little effect on the duration and appearance of the lag period. The time required for consumption of half of the added *p*-benzoquinone increased slightly, to 18 min.

Results presented in Fig. 5b, performed in the presence of 5 μM EDTA, can be compared with results obtained under EDTA-free conditions (Fig. 4a). The added EDTA eliminated the lag period and raised the rate of *p*-benzoquinone consumption. The time required for consumption of half of the added *p*-benzoquinone dropped to approximately 6 min.

Time courses for six additional pH values, presented in Fig. 6, can be compared with the results presented in Fig. 4a. Lag periods were observed in the experiments performed at pH 5.4, 5.7, 5.8, 5.9, and 6.1, but not in experiments performed at pH 5.6 and 6.3. The lack of correlation between pH and lag period, even among experiments performed using the same pH buffer, is important to note. Increasing the pH generally decreased the time required for consumption of half of the added *p*-benzoquinone. At pH 5.4, an hour was required, while at pH 6.3, only a few minutes were required.

3.2 Substituted *p*-Benzoquinones

As shown in Figs. 7 and 8, lag periods and less-pronounced S-shaped curves are common features of time course plots obtained with substituted *p*-benzoquinones. To capture comparable reaction progress intervals, *p*-benzoquinones bearing electron-withdrawing groups (e.g. –Cl) required more acidic pH conditions, while those with electron-donating groups (–C_6H_5, –CH_3, –OCH_3) required more alkaline pHs. Single-ring substrates (e.g. methyl-*p*-benzoquinone) required more acidic pHs than dual-ring substrates (*p*-naphthoquinone). Times required for consumption of half of added *p*-benzoquinone consistently and dramatically decreased as the experimental pH was increased.

For comparison purposes, reaction rates have been calculated using slopes of benzoquinone concentration versus time plots. Data points collected after the lag period but before the point corresponding to 30% benzoquinone consumption were employed. As

Fig. 5 Time course plots when **a** 94 μM pre-formed Fe^{III} (hydr)oxide and **b** 5 μM EDTA are present at the onset of reaction. Reaction conditions: 50 μM *p*-benzoquinone, 250 μM Fe^{II}, 50 mM MES pH buffer (pH 5.9), and 0.10 M NaCl
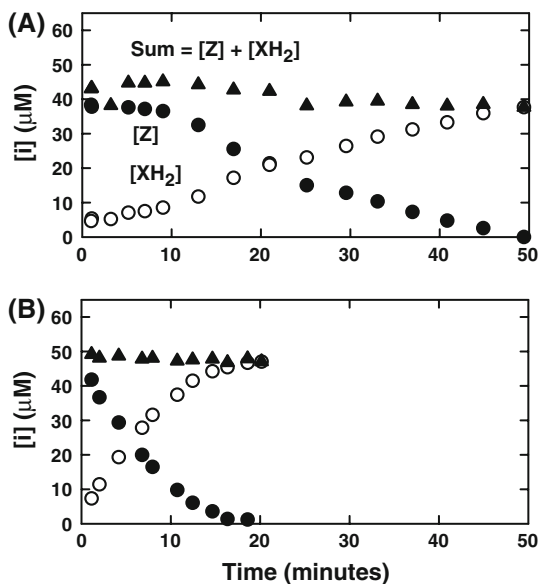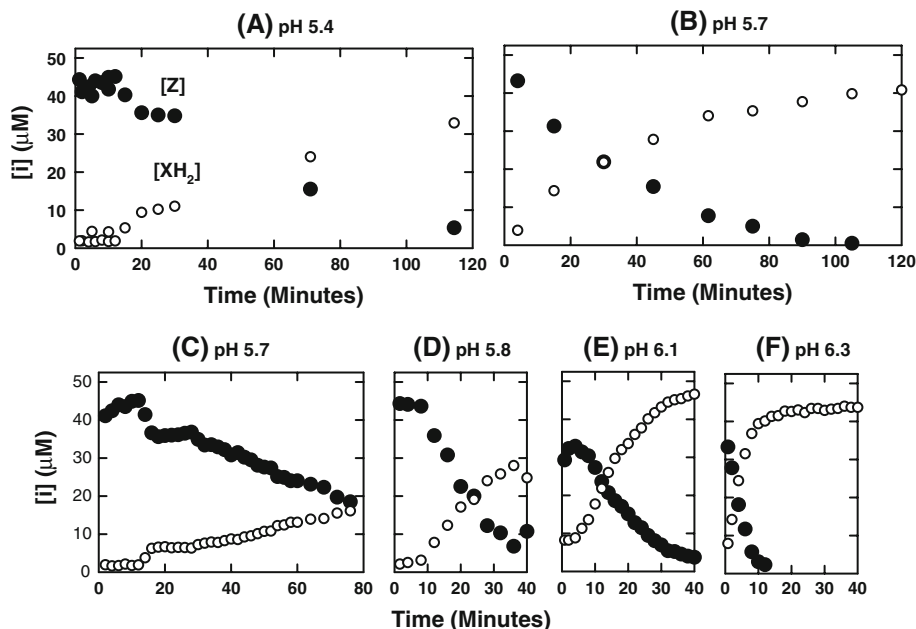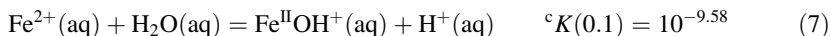
Fig. 6 Time course plots for the reduction in 50 μM *p*-benzoquinone by 250 μM Fe^{II}·10 mM Acetate buffer was used in **a** and 10 mM MES buffer was used in **b**–**f**. All suspensions contained 0.10 M NaCl

Fig. 9 indicates, rates increased with increasing pH. If we suppose that each rate is proportional to $[H^+]^n$, then the order n can be found from the slope of log(rate) plotted as a function of log[H$^+$]. Values of n ranged from −0.98 for *p*-naphthoquinone to −2.70 for phenyl-*p*-benzoquinone. Figure 9 also notes the pH required for a benzoquinone consumption rate of $10^{-7.5}$ M s^{-1} to be achieved. Electron-withdrawing constituents (–Cl) shifted this point toward more acidic pHs, while electron-donating substituents (–C$_6$H$_5$, –CH$_3$, –OCH$_3$) caused a shift toward more alkaline pHs. *p*-Naphthoquinone, the substrate with the lowest E^o, required the highest pH for this rate to be achieved. It should be noted that among the six substrates, unsubstituted *p*-benzoquinone yielded the highest amount of experiment-to-experiment variability in rate.

4 Discussion

4.1 Reaction Energetics

The benzoquinones included in this study do not possess pK$_a$s for either protonation or deprotonation within the range 0 < pH < 14. We can conclude that Z^o(aq) serves as the reactive species. Equilibrium constants from Martell et al. (2004), corrected for the 0.10 M NaCl ionic medium used in our experiments, reveal potentially relevant Fe^{II} species:
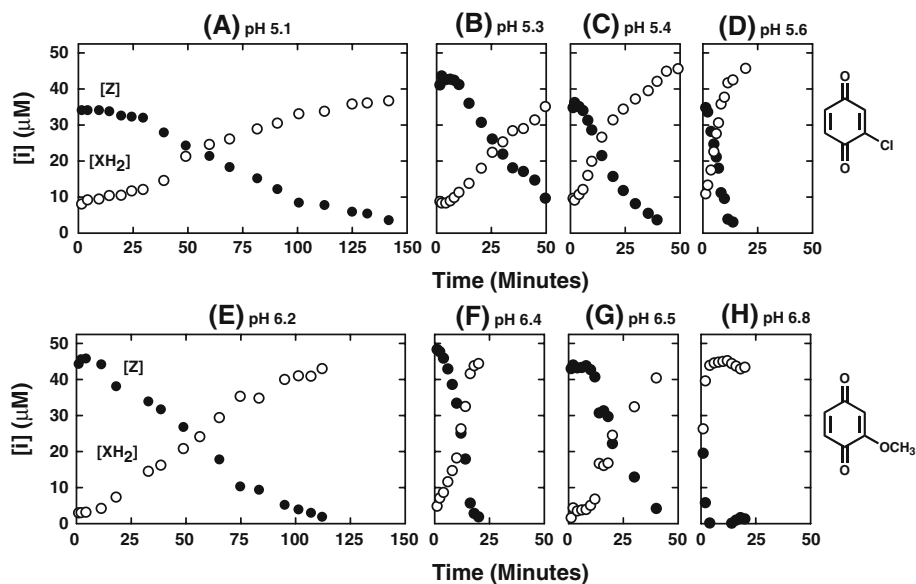
$$Fe^{2+}(aq) + Cl^-(aq) = Fe^{II}Cl^+(aq) \qquad {}^cK(0.1) = 10^{-0.72} \qquad (6)$$

$$Fe^{2+}(aq) + H_2O(aq) = Fe^{II}OH^+(aq) + H^+(aq) \qquad {}^cK(0.1) = 10^{-9.58} \qquad (7)$$

Fig. 7 Time course plots for the reduction in 50 μM chloro-*p*-benzoquinone (**a–d**) and 50 μM methoxy-*p*-benzoquinone (**e–h**) by 250 μM Fe^{II}. 10 mM Acetate buffer was used in **a–c**, 10 mM MES buffer in **d–f**, and 10 mM MOPS in **g–h**. All suspensions contained 0.10 M NaCl
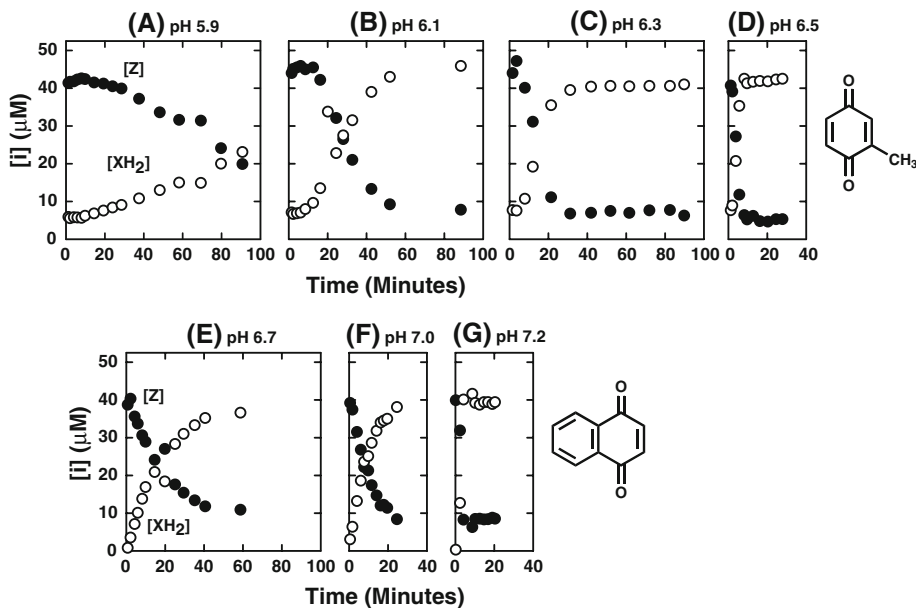

Fig. 8 Time course plots for the reduction in 50 μM methyl-*p*-benzoquinone (**a–d**) and 50 μM *p*-naphthoquinone (**e–g**) by 250 μM Fe^{II}. 10 mM MES buffer was used in **a–c**, and 10 mM MES buffer in **d–g**. All suspensions contained 0.10 M NaCl
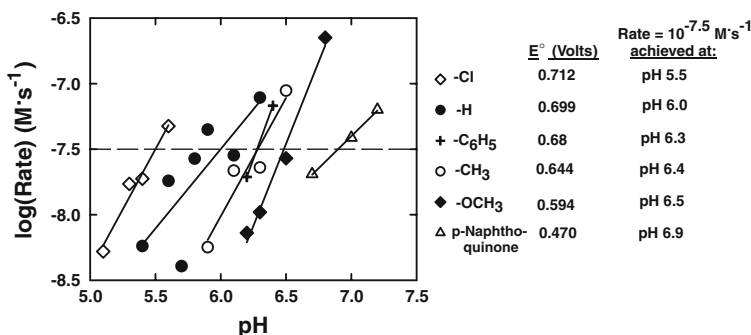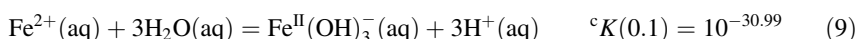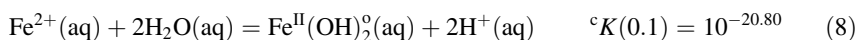
Fig. 9 Log rates as a function of pH for the reduction in six substituted *p*-benzoquinones by Fe^{II}. Reaction conditions: 50 μM *p*-benzoquinone, 250 μM Fe^{II}, 50 mM pH buffer, and 0.10 M NaCl

$$Fe^{2+}(aq) + 2H_2O(aq) = Fe^{II}(OH)_2^o(aq) + 2H^+(aq) \qquad {}^cK(0.1) = 10^{-20.80} \qquad (8)$$

$$Fe^{2+}(aq) + 3H_2O(aq) = Fe^{II}(OH)_3^-(aq) + 3H^+(aq) \qquad {}^cK(0.1) = 10^{-30.99} \qquad (9)$$

An additional relevant equilibrium constant has been reported by Morel and Hering (1993):

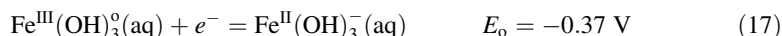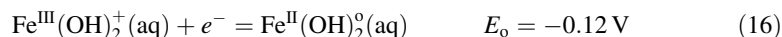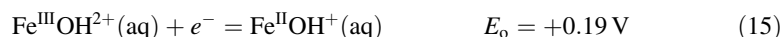$$Fe^{2+}(aq) + Acetate^-(aq) = Fe^{II}Acetate^+(aq) \qquad {}^cK(0.1) = 10^{+0.98} \qquad (10)$$
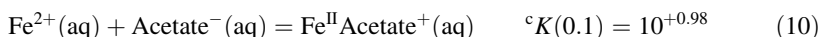
The first electron transfer step, converting $Z^o(aq)$ into semiquinone radical species, is likely rate limiting. Benzoquinone loss should obey the following rate equation:

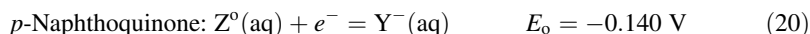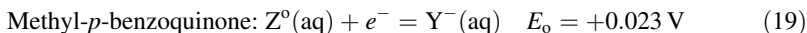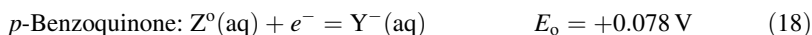$$\frac{-d[Z]}{dt} = k_0[Fe^{2+}][Z] + k_{Cl}[Fe^{II}Cl^+][Z] + k_{Acetate}[Fe^{II}Acetate^+][Z] + k_1[Fe^{II}OH^+][Z]$$
$$+ k_2\left[Fe^{II}(OH)_2^o(aq)\right][Z] + k_3\left[Fe^{II}(OH)_3^-\right][Z] \qquad (11)$$

The dominant term is a function of the species concentration times the corresponding rate constant. For reaction with Fe^{II}Cl$^+$(aq) to be as important as reaction with Fe^{2+}(aq), k_{Cl} would have to be 52-times larger than k_0. At pH 6.0, k_1 would have to be 4.9×10^3 times greater than k_o for reaction with Fe^{II}OH$^+$(aq) to be as significant as reaction with Fe^{2+}(aq). Similarly, k_2 and k_3 would have to be 1.0×10^9 and 2×10^{13} times larger than k_o for reaction with Fe^{II}(OH)$_2^o$(aq) and Fe^{II}(OH)$_3^-$(aq) to be significant.

The standard approach toward addressing the energetics of Fe^{III}/Fe^{II} interconversion is to compare reduction potentials (e.g. Strathmann and Stone 2002). According to the Franck–Condon principle (IUPAC 1997), protons and other nuclei are stationary during electron transfer. Hence, the following half reactions are appropriate:

$$Fe^{3+}(aq) + e^- = Fe^{2+}(aq) \qquad\qquad E_o = +0.77\,V \qquad (12)$$

$$Fe^{III}Cl^{2+}(aq) + e^- = Fe^{II}Cl^+(aq) \qquad\qquad E_o = +0.67\,V \qquad (13)$$

$$Fe^{III}Acetate^{2+}(aq) + e^- = Fe^{II}Acetate^+(aq) \quad E_o = +0.62\,V \qquad (14)$$

$$Fe^{III}OH^{2+}(aq) + e^- = Fe^{II}OH^+(aq) \qquad\qquad E_o = +0.19\,V \qquad (15)$$

$$Fe^{III}(OH)_2^+(aq) + e^- = Fe^{II}(OH)_2^o(aq) \qquad E_o = -0.12\,V \qquad (16)$$

$$Fe^{III}(OH)_3^o(aq) + e^- = Fe^{II}(OH)_3^-(aq) \qquad E_o = -0.37\,V \qquad (17)$$

(Note that infinite dilution scale reduction potentials are employed). Unfortunately, one-electron reduction potentials (Wardman 1989) are only available for only three of the six of the benzoquinones that were investigated. We denote protonated and deprotonated semiquinone radicals as $HY^{\cdot}(aq)$ and $Y^{-}(aq)$, respectively:

$$p\text{-Benzoquinone: } Z^o(aq) + e^- = Y^-(aq) \qquad E_o = +0.078 \text{ V} \qquad (18)$$

$$\text{Methyl-}p\text{-benzoquinone: } Z^o(aq) + e^- = Y^-(aq) \quad E_o = +0.023 \text{ V} \qquad (19)$$

$$p\text{-Naphthoquinone: } Z^o(aq) + e^- = Y^-(aq) \qquad E_o = -0.140 \text{ V} \qquad (20)$$

Comparisons of reduction potentials lead to two important conclusions. First, formation of Fe^{II} (hydr)oxo species is necessary to make the first electron transfer step energetically favorable. Second, decreases in reaction rate in going from p-benzoquinone to methyl-p-benzoquinone and p-naphthoquinone follow the same trend as decreases in ΔG for the forward reaction, calculated using Eq. 5.

Fe^{II} speciation is relevant to the effect of pH on reaction rate. Within the pH range of our experiments, $[Fe^{2+}(aq)]$ is invariant as the pH is increased. Mass action expressions based on Eqs. 7–9 can be used to show that $[Fe^{II}OH^+(aq)]$ is proportional to $[H^+]^{-1}$, $[Fe^{II}(OH)_2^o(aq)]$ proportional to $[H^+]^{-2}$, and $[Fe^{II}(OH)_3^-(aq)]$ proportional to $[H^+]^{-3}$. Steep increases in rate as the pH is increased are in accord with Fe^{II} hydroxo species serving as principal reductant species.

Semiquinone radicals undergo protonation reactions, i.e., $YH = Y^-(aq) + H^+(aq)$. The pK_a for p-benzosemiquinone is 4.0, while the methyl-substituted form and naphthyl form have pK_as of 4.5 and 4.1, respectively (Steenken and Neta 2003). The pK_a for chloro-p-benzosemiquinone is believed to be approximately one log unit below that of p-benzosemiquinone (Fukuzumi et al. 1987). YH/Y^- are likely consumed rapidly by Fe^{II}. Within the pH range of our experiments, re-reduction in $Z^o(aq)$ by Fe^{III} species is not believed to be significant.

4.2 Time Course Behavior

Lag periods and S-shaped curves observed in many of our time course plots indicate that a reaction intermediate or product promotes the forward reaction. Experiment-to-experiment variability in lag period duration and substrate consumption rates indicates that a low concentration species is playing a disproportionately large role in the reaction mechanism.

Based upon energetic considerations, reaction rate increases accompanying Fe^{II} adsorption to Fe^{III} (hydr)oxide particles would be entirely reasonable. From both thermodynamic and kinetic perspectives, the adsorbed species $(> Fe^{III}OFe^{II})^+$ and $(> Fe^{III}OFe^{II}OH)^o$ are analogous in many respects to the Fe^{II} (hydr)oxo species in solution described earlier (Wehrli 1990). Previously, Fe^{II} adsorption onto (hydr)oxides has been shown to accelerate the reduction in nitrobenzenes (Klausen et al. 1995), oxime carbamates (Strathmann and Stone 2003), carbon tetrachloride (Amonette et al. 2000), and other polyhalogenated methanes (Pecher et al. 2002). In our experiments, however, adding pre-formed Fe^{III} (hydr)oxide particles had very little effect on p-benzoquinone reduction. We can only conclude that pH and (hydr)oxide area loadings were too low for Fe^{II} adsorption to have a significant effect on rate.

Chelating agents with higher logKs for complex formation with Fe^{III} than for Fe^{II} accelerate Fe^{II} oxidation (Buerge et al. 1998; King and Farlow 2000; Wehrli et al. 1989; Wehrli 1990; Strathmann and Stone 2002). The effect is explained by evoking stabilization

of the transition state, which has some Fe^{III} product character (Purcell and Kotz 1977). p-Benzoquinone is a very poor Lewis base. Coordination of Fe^{II} by carbonyl oxygen atoms of p-benzoquinone makes possible electron transfer via an inner sphere mechanism, but would do little to change the energetics of Fe^{II} oxidation. Despite its two phenolic groups, hydroquinone can only serve as a monodentate ligand. Fe^{II} must compete with protons for coordination of the phenolate anion, which possesses a p^aK_a of 10.11 (Martell et al. 2004). Accordingly, the extent of Fe^{II} coordination by hydroquinone is unlikely to be a factor in determining reaction rate. It can also be noted that, based on previous adsorption studies (Vasudevan and Stone 1998), significant adsorption of hydroquinone and p-benzoquinone onto Fe^{III} (hydr)oxide surfaces generated during the reaction is unlikely to occur.

EDTA, of course, is a very strong chelating agent. The equilibrium constant for the complexation of Fe^{III} by EDTA is $10^{10.8}$-times higher than the corresponding constant for the complexation of Fe^{II} (Martell et al. 2004). It makes sense that 5 μM EDTA had a significant effect on reaction kinetics. In addition to lowering the activation energy barrier to Fe^{II} oxidation, EDTA is likely to slightly delay the onset of Fe^{III} (hydr)oxide precipitation. Chelating agent effects on reaction progress will be examined in greater detail in a separate publication.

Calculations presented in Fig. 3b indicate that adding hydroquinone lowers ΔG at the onset of Fe^{2+}(aq) reduction by p-benzoquinone. The ΔG diminishment becomes less significant as the reaction progresses. Although the experiments presented in Fig. 4 were performed under different conditions, i.e., higher $[Fe^{2+}(aq)]$ and pH, the same conclusions apply. Quinhydrone formation ($Z^o + XH_2^o = Z,XH_2$) and comproportionation ($Z^o + XH_2^o = 2YH^\cdot$) are additional factors to consider (Roginsky et al. 1999; Tossell 2009). Equilibrium constants for both reactions strongly favor reactants over products (Uchimiya and Stone 2006). For this reason, they are not likely to lead to any significant decrease in the p-benzoquinone concentration available for reduction by Fe^{2+}(aq).

5 Conclusions

O_2(aq), $O_2^{\bullet-}$, H_2O_2, $OH^\bullet$, NO_3^-(aq), NO_2^-(aq), N_2O(aq), and $Mn^{III,IV}$ (hydr)oxides all occur naturally and oxidize Fe^{II} when prevalent chemical conditions are appropriate. A number of synthetic organic contaminants, noted earlier, also oxidize Fe^{II}. Here, we add an important class of natural products to this list, the benzoquinones.

Dihydroxynapthalenes and dihydroxyanthracenes possess adjoining aromatic rings. As a consequence, such compounds exhibit reduction potentials favorable for Fe^{III} reduction, making them suitable electron shuttling agents for bacterial Fe^{III} (hydr)oxide respiration. Single-ring benzoquinone/dihydroxybenzenes, in contrast, exhibits reduction potentials favorable for Fe^{II} oxidation. Biogeochemists should be alerted to the fact that benzoquinone/dihydroxybenzene natural products exuded by different organisms may work at cross purposes to one another. As structures of new benzoquinone/dihydroxybenzene natural products are discovered, the chemical approaches employed here can aid in evaluating their putative biogeochemical roles.

References

Alegria AE, Lopez M, Guevara N (1996) Thermodynamics of semiquinone disproportion in aqueous buffer. J Chem Soc Faraday Trans 92:4965–4968

Amonette JE, Workman DJ, Kennedy DW, Fruchter JS, Gorby YA (2000) Dechlorination of carbon tetrachloride by Fe(II) associated with goethite. Environ Sci Technol 34:4606–4613

Arnold RG, Olson TM, Hoffmann MR (1986) Kinetics and mechanism of dissimilative Fe(III) reduction by *Pseudomonas* sp. 200. Biotechnol Bioeng 28:1657–1671

Baxendale JH, Hardy HR (1955) Kinetics and equilibria in solutions containing ferrous ion, ferric ion, and some substituted hydroquinones and Quinones. Trans Farad Soc 50:808–814

Baxendale JH, Hardy HR, Sutcliffe LH (1951) Kinetics and equilibria in the system ferrous ion + ferric ion + hydroquinone. Trans Farad Soc 47:963–973

Bespalov VA, Zhulin IB, Taylor BL (1996) Behavioral responses of *Escherichia coli* to changes in redox potential. Proc Natl Acad Sci USA 93:10084–10089

Buerge IJ, Hug SJ (1998) Influence of organic ligands on chromium(VI) reduction by iron(II). Environ Sci Technol 32:2092–2099

Cervantes FJ, Duong-Dac T, Roest K, Akkermans ADL, Lettinga G, Field JA (2003) Enrichment and immobilization of quinone-respiring bacteria in anaerobic granular sludge. Water Sci Technol 48:9–16

Chang M, Netzly DH, Butler LG, Lynn DG (1986) Chemical regulation of distance: characterization of the first natural host germination stimulant for *Striga asiatica*. J Am Chem Soc 108:7858–7860

Coates JD, Ellis DJ, Blunt-Harris EL, Gaw CV, Roden EE, Lovley DR (1998) Recovery of humic-reducing bacteria from a diversity of environments. Appl Environ Microbiol 64:1504–1509

Cory RM, McKnight DM (2005) Fluorescence spectroscopy reveals ubiquitous presence of oxidized and reduced quinones in dissolved organic matter. Environ Sci Technol 39:8142–8149

Fimmen RL, Cory RM, Chin Y-P, Trouts TD, McKnight DM (2007) Probing the oxidation-reduction properties of terrestrially and microbially derived dissolved organic matter. Geochim Cosmochim Acta 71:3003–3015

Fukuzumi S, Ishikawa K, Hironaka K, Tanaka T (1987) Acid catalysis in thermal and photoinduced electron-transfer reactions. J Chem Soc Perkin Trans 2:751–760

Gonzalez VM, Kazimir J, Nimbal C, Weston LA, Cheniae GM (1997) Inhibition of a Photosystem II electron transfer reaction by the natural product sorgoleone. J Agric Food Chem 45:1415–1421

Good NE, Izawa S (1972) Hydrogen ion buffers. Meth Enzymol 24:53–68

Good NE, Winget GD, Winter W, Connolly TN, Izawa S, Singh RMM (1966) Hydrogen ion buffers for biological research. Biochemistry 5:467–477

Haas JR, DiChristina TJ (2002) Effects of Fe(III) chemical speciation on dissimilatory Fe(III) reduction by *Shewanella putrefaciens*. Environ Sci Technol 36:373–380

Hejl AM, Koster KL (2004) Juglone disrupts root plasma membrane H^+-ATPase activity and impairs water uptake, root respiration, and growth in soybean (*Glycine max*) and corn (*Zea mays*). J Chem Ecol 30:453–471

Hernandez ME, Kappler A, Newman DK (2004) Phenazines and other redox-active antibiotics promote microbial mineral reduction. Appl Environ Microbiol 70:921–928

IUPAC (1997) Compendium of chemical terminology, 2nd edn. Compiled by McNaught AD, Wilkinson A. Blackwell, Oxford

Jiang J, Kappler A (2008) Kinetics of microbial and chemical reduction of humic substances: implications for electron shuttling. Environ Sci Technol 42:3563–3569

Johnson HA, Tebo BM (2008) In vitro studies indicate a quinone is involved in bacterial Mn(II) oxidation. Arch Microbiol 189:59–69

King DW, Farlow R (2000) Role of carbonate speciation on the oxidation of Fe(II) by H_2O_2. Mar Chem 70:201–209

Klapper L, McKnight DM, Fulton JR, Blunt-Harris EL, Nevin KP, Lovley DR, Hatcher PG (2002) Fulvic acid oxidation state detection using fluorescence spectroscopy. Environ Sci Technol 36:3170–3175

Klausen J, Troeber SP, Haderlein SB, Schwarzenbach RP (1995) Reduction of substituted nitrobenzenes by Fe(II) in aqueous mineral suspensions. Environ Sci Technol 29:2396–2404

Lies DP, Hernandez ME, Kappler A, Mielke RE, Gralnick JA, Newman DK (2005) Shewanella oneidensis MR-1 uses overlapping pathways for iron reduction at a distance and by direct contact under conditions relevant for biofilms. Appl Environ Microbiol 71:4414–4426

Linert W, Herlinger E, Jameson RF (1993) A kinetic study of the anaerobic reactions between adrenaline and iron(III). J Chem Soc Perkin Trans 2:2435–2439

Lovley DR, Coates JD, Blunt-Harris EL, Phillips EJP, Woodward JC (1996) Humic substances as electron acceptors for microbial respiration. Nature 382:445–448

Lovley DR, Fraga JL, Blunt-Harris EL, Hayes LA, Phillips EJP, Coates JD (1998) Humic substances as a mediator for microbially catalyzed metal reduction. Acta Hydrochim Hydrobiol 26:152–157

Lovley DR, Fraga JL, Coates JD, Blunt-Harris EL (1999) Humics as an electron donor for anaerobic respiration. Environ Microbiol 1:89–98

Majzlan J, Navrotsky A, Schwertmann U (2004) Thermodynamics of iron oxides: part III. Enthalpies of formation and stability of ferrihydrite (Fe(OH)$_3$), schwertmannite (FeO(OH)$_3$/4(SO$_4$)1/8) and ε-Fe$_2$O$_3$. Geochim Cosmochim Acta 68:1049–1059

Martell AE, Smith RM, Motekaitis RJ (2004) NIST critically selected stability constants of metal complexes, version 8.0, NIST Standard Database 46. NIST, Gaithersburg, MD

Mentasti E, Pelizzetti E, Saini G (1973) Reactions between iron (III) and catechol (o-dihydroxybenzene). Part II. Equilibria and kinetics of the redox reaction in aqueous acid solution. J Chem Soc Dalton Trans (23):2609–2614

Morel FMM, Hering JG (1993) Principles and applications of aquatic chemistry. Wiley, New York

Newman DK, Kolter R (2000) A role for excreted quinones in extracellular electron transfer. Nature 405:94–97

Nurmi JT, Tratnyek PG (2002) Electrochemical properties of natural organic matter (NOM), fractions of NOM, and biogeochemical electron shuttles. Environ Sci Technol 36:617–624

Paul A, Stosse R, Zehl A, Zwirnmann E, Vogt RD, Steinberg CEW (2006) Nature and abundance of organic radicals in natural organic matter: effect of pH and irradiation. Environ Sci Technol 40:5897–5903

Pecher K, Haderlein SB, Schwarzenbach RP (2002) Reduction of polyhalogenated methanes by surface-bound Fe(II) in aqueous suspensions of iron oxides. Environ Sci Technol 36:1734–1741

Pezzella A, d'Ischia M, Napolitano A, Misuraca G, Prota G (1997) Iron-mediated generation of the neurotoxin 6-hydroxydopamine quinone by reaction of fatty acid hydroperoxides with dopamine: a possible contributory mechanism for neuronal degeneration in Parkinson's Disease. J Med Chem 40:2211–2216

Porret D (1934) Oxidation of ferrous sulfate by quinone and the reverse reaction. Helv Chim Acta 17:703–716

Purcell KF, Kotz JC (1977) Inorganic chemistry. W.B. Saunders, Philadelphia

Roginsky VA, Pisarenko LM, Bors W, Michel C (1999) The kinetics and thermodynamics of quinone-semiquinone-hydroquinone systems under physiological conditions. J Chem Soc Perkin Trans 2:871–876

Schwarzenbach RP, Stierli R, Lanz K, Zeyer J (1990) Quinone and iron porphyrin mediated reduction of nitroaromatic compounds in homogeneous aqueous solution. Environ Sci Technol 24:1566–1574

Scott DT, McKnight DM, Blunt-Harris EL, Kolesar SE, Lovley DR (1998) Quinone moieties act as electron acceptors in the reduction of humic substances by humics-reducing microorganisms. Environ Sci Technol 32:2984–2989

Senesi N, Steelink C (1989) Application of ESR spectroscopy to the study of humic substances, chap 13. In: Hayes MHB, MacCarthy P, Malcolm RL, Swift RS (eds) Humic substances II. Wiley, NY, pp 373–378

Steenken S, Neta P (2003) Transient phenoxy radicals: formation and properties in aqueous solutions. In: Rappoport Z (ed) The chemistry of phenols. Wiley, NY, pp 1107–1152

Strathmann TJ, Stone AT (2002) Reduction of oxamyl and related pesticides by Fe^{II}: influence of organic ligands and natural organic matter. Environ Sci Technol 36:5172–5183

Strathmann TJ, Stone AT (2003) Mineral surface catalysis of reactions between Fe^{II} and oxime carbamate pesticides. Geochim Cosmochim Acta 67:2775–2791

Stumm W, Morgan JJ (1996) Aquatic chemistry. Chemical equilibria and rates in natural waters. Wiley, NY

Thorn KA, Pettigrew PJ, Goldenberg WS, Weber EJ (1996) Covalent binding of aniline to humic substances. 2. 15 N NMR studies of nucleophilic addition reactions. Environ Sci Technol 30:2764–2775

Tossell JA (2009) Quinone-hydroquinone complexes as model components of humic acids: theoretical studies of their structure, stability and visible–UV spectra. Geochim Cosmochim Acta 73:2023–2033

Uchimiya M, Stone AT (2006) Redox reactions between iron and quinones: thermodynamic constraints. Geochim Cosmochim Acta 70:1388–1401

Vasudevan D, Stone AT (1998) Adsorption of 4-nitrocatechol, 4-nitro-2-aminophenol, and 4-nitro-1, 2-phenylenediamine at the metal (hydr)oxide/water interface: effect of metal (hydr)oxide properties. J Colloid Interface Sci 202:1–19

von Jagow G, Link TA (1986) Use of specific inhibitors on the mitochondrial bc$_1$ complex. Meth Enzymol 126:253–271

Wardman P (1989) Reduction potentials of one-electron couples involving free radicals in aqueous solution. J Phys Chem Ref Data 18:1637–1756

Wehrli B (1990) Redox reactions of metal ions at mineral surfaces. In: Stumm W (ed) Aquatic chemical kinetics. Wiley, NY, pp 311–336

Wehrli B, Sulzberger B, Stumm W (1989) Redox processes catalyzed by hydrous oxide surfaces. Chem Geol 78:167–179